Front. Optoelectron. 2018, 11(1): 30–36
https://doi.org/10.1007/s12200-018-0762-8

REVIEW ARTICLE

Dipole-fiber system: from single photon source to metadevices

Shaghik ATAKARAMIANS (✉)[1], Tanya M. MONRO[2,3], Shahraam AFSHAR V.[2,3]

1 School of Electrical Engineering and Telecommunications, The University of New South Wales, Sydney, NSW 2052, Australia
2 Institute for Photonics and Advanced Sensing, The University of Adelaide, Adelaide SA 5005, Australia
3 Laser Physics and Photonic Devices Laboratories, School of Engineering, University of South Australia, Mawson Lakes SA 5095, Australia

Abstract Radiation of an electric dipole (quantum emitter) in vicinity of optical structures still attracts great interest due to emerging of novel application and technological advances. Here we review our recent work on guided and radiation modes of electric dipole and optical fiber system and its applications from single photon source to metadevices. We demonstrate that the relative position and orientation of the dipole and the core diameter of the optical fiber are the two key defining factors of the coupled system application. We demonstrate that such a coupled system has a vast span of applications in nanophotonics; a single photon source, a high-quality factor sensor and the building block of metadevices.

Keywords dipole source, optical fibers, single photon source, whispering gallery modes, electric and magnetic response

1 Introduction

Radiation of a dipole or a quantum emitter in vicinity of optical structures is a fundamental field of research that has been extensively studied both theoretically and experimentally [1–3] and Ref. therein, and utilized in many applications including different sensing mechanisms [4–6], photonic band-gap devices [7,8], nonlinear optics [9,10], superscatteres [11], antenna [12–14], metadevices [15,16]. The field still attracts significant interests, first, due to technological advances that have led to new possibilities for fabricating nanoscale optical structures that can be doped or coated with nanoparticles with variety of different optical properties. Secondly, there are now advanced techniques to excite "optical modes" using phase-matched optical waveguides, and fluorescence emission of incorporated or coated nanoparticles. Finally, novel applications of the concept of dipole-optical structures are emerging. Optical fibers are one of the important class of optical structures since they provide two types of interactions; dipole-guided and dipole-radiation modes interactions [2,17,18]. Each of these interactions has unique and distinct properties, making them suitable for different applications.

Here, we summarize our work on the interaction of optical fibers with a point source, i.e., an electric dipole in classical regime and quantum emitter in quantum mechanics. We demonstrate that such a coupled system has a vast span of applications; a single photon source [19–21], a high-quality factor sensor [2] and can be the building block of metadevices [22,23]. We first give a brief summary of the theory of dipole-fiber system in Section 2. This is followed by a summary of the experimental efforts, in Section 3, to implement a practical dipole-fiber system in which a step index tellurite optical fiber is doped with diamond nanoparticles with nitrogen vacancy centers in order to develop a guided single photon source. In Section 4, we focus on the origin and properties of radiation modes of an optical fiber. Using the theory reviewed in Section 2 and numerical simulations, we show how the radiation of a dipole can be coupled into these radiation modes. In particular we show that higher order radiation modes have large Q, and high sensitivity to the refractive index of the environment around the optical fiber. In Section 5, the lowest order radiation modes are expanded in terms of their electric and magnetic dipole contributions. It is shown theoretically that for a certain dipole orientation, the radiation modes resemble strong enhanced magnetic responses. Such a strong magnetic response can be used as building block of metamaterials and metadevices.

Received September 30, 2017; accepted January 19, 2018

E-mail: s.atakaramians@unsw.edu.au

2 Theory

The interaction of a dipole with an optical fiber, in general, can be described using Green's function [24] or modal decomposition method [2,18]. We use modal decomposition method since it allows us to separately consider the contribution of guided and radiation modes. We model the point source, which can be an electric transition in an atom or electric dipole source, with a dipole moment p_0 oscillating with a frequency ω. The fiber is modeled as an infinitely long dielectric cylinder of radius r_{co} and refractive index n_{co} surrounded by an infinite region of air cladding ($n_{cl} = 1$). In the examples presented in the following sections, we have considered tellurite glass as the core material ($n_{co} \approx 2.025$) and $\lambda = 700$ nm as the operating wavelength of dipole emission, which represents the single atom emission of diamond centers [19]. The total field emitted by the dipole and optical fiber system can be written as [17,18]

$$\begin{aligned}\boldsymbol{E}(x,y,z) = & \sum_j a_j \boldsymbol{e}_j(x,y)\mathrm{e}^{\mathrm{i}\beta_j z} \\ & + \sum_\nu \int_0^{Q_{\max}} a_\nu(Q) e_\nu(x,y,Q)\mathrm{e}^{\mathrm{i}\beta_\nu(Q)z}\mathrm{d}Q \\ & + BK, \end{aligned} \tag{1}$$

where a_j, $a_\nu(Q)$ and $\boldsymbol{e}_j(x,y)$, $\boldsymbol{e}_\nu(x,y,Q)$ are coupling coefficients and modal vector fields for forward guided and radiation modes, respectively, j and ν are respectively the azimuthal guided and radiation mode indices, β_j's are the corresponding propagation constants, $Q = (D/2)(k^2 n_{cl}^2 - \beta^2)^{1/2}$, D is the core diameter, $k = 2\pi/\lambda$, and BK represents the contribution of backward guided and radiation modes. Note that the guided and radiation modes are orthogonal to each other and the discrete and continuous values of the propagation constants β of these modes, respectively, are $kn_{cl} \leqslant \beta_j \leqslant kn_{co}$ for guided modes and $0 \leqslant \beta \leqslant kn_{cl}$ for radiation modes. The coupling coefficients a_j and a_ν are [17,18]

$$|a_{j,\nu}|^2 = \frac{\omega^2}{16N_{j,\nu}^2}|\boldsymbol{e}_{j,\nu}^*(\boldsymbol{r}_0)\cdot \boldsymbol{p}_0(\boldsymbol{r}_0)|^2, \tag{2}$$

where $N_{j,\nu} = \left(\frac{1}{2}\right)\int_{A-\infty}^{A+\infty}(e_{j,\nu} \times h_{j,\nu}^*)\cdot \hat{z}\mathrm{d}A$ is the normalization term. The power captured in each guided and radiated modes are $P_j = |a_j|^2 N_j$ and $P_\nu = |a_\nu|^2 N_\nu$, respectively. Hence the total emitted power of the dipole-waveguide system is the sum of the power captured into all guided and radiation modes as follows [2,17,18]:

$$P_{\text{total}} = \sum_j P_j + \sum_\nu \int_0^{Q_{\max}} P_\nu(Q)\mathrm{d}Q. \tag{3}$$

3 Photon collection platform for quantum mechanics

Quantum-base technology has been identified as a potential disruptive technology of twenty first century. A building block of such a technology consists of devices that operate at quantum-classic interface. One important class of these devices combine quantum emitters with photonic structures. They allow quantum information to be integrated to photonic modes of the structure, which in turn allows read-in, read-out connections with the quantum emitters.

In recent years, diamond nanocrystals containing nitrogen vacancy (NV) centers have become one of the important platforms to exhibit room-temperature quantum effects [19]. The fluorescence emission of these centers exhibits a characteristic single photon statistic. We have demonstrated, with careful fabrication process [19–21], that diamond nanoparticles with NV centers can be doped within tellurite glass structure, which can then be pulled into optical fibers, see Fig. 1(a). Exciting the NV centers

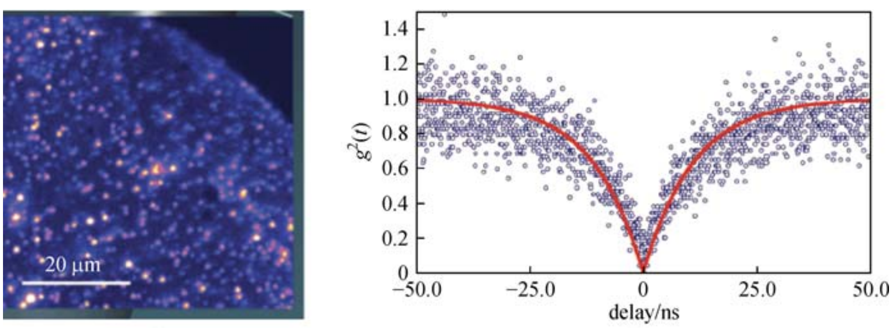

(a) (b)

Fig. 1 (a) Diamond optical fiber excited at the endface using 700 nm laser. (b) Background corrected measured second order autocorrelation function (blue circles) of a single NV–center embedded in the tellurite optical fiber. The solid red line represents a single exponential fit of the photon statistics Both parts adapted from Ref. [19]

within the optical fiber and measuring and examining the statistical characteristics of their fluorescence emission show the antibunching behavior, characteristic of single photon emission, see Fig. 1(b). The success in embedding NV centers within optical fibers without losing their single photon emission properties is an important step toward a hybrid quantum-classic platform. The NV centers within optical fibers can be excited through guided modes of the fiber and their fluorescence single photon emission can then be captured into guided modes. This forms a robust configuration to develop guided single photon sources for quantum applications.

We can use the theoretcial model discussed in Section 2 to study and enhance the collection efficiency into the guided modes of the optical fiber [18]. The fraction of power coupled into guided modes of the optical power can be determined from the first term (P_j) in Eq. (3). The total power captured in guided modes by a dipole located in the center (labeled 'center') and at the core-cladding interface (labeled 'interface') of a tellurite fiber is shown in Fig. 2. The captured power has been normalized to the total power emitted by a dipole in bulk diamond. We find that the power captured into the guided modes of the fiber depends on the location of the source in the core and can be greater than the total emitted power of a dipole in bulk diamond. In generally, for many core diameters and dipole positions, the power captured is greater than 20% of the power emitted in bulk diamond and it is typically higher for a radially oriented dipole (~50%–60%) [18]. The discontinuities in the plots are due to the appearance of new guided modes as the core diameter is increased.

4 Ultra-sensitive platform for sensing

In Section 3, we considered photon collection into the guided modes of the optical fiber and studied the effect of dipole orientation and position on the collection efficiency. In this section, we investigate the effect of dipole emission into radiation modes of the optical fiber [2,22]. We consider dipole sitting at the core-cladding interface, and we theorectically study the role of dipole orientation on the radiation modes, where strong resonance peaks are observed due to formation of whispering gallery modes (WGMs) at the fiber cross section.

The total radiated power of the coupled system is calculated using Eq. (3), where the total power is the sum of radiation modes of the fiber integrated over the continuous propagation constant of radiation modes. It is worth mentioning that similar to guided modes, radiation modes are also formed by the superposition of TE- and TM-like modes (relatively small longitudinal electric and magnetic fields, respectively) [17]. The contribution of each of these TE- and TM-like modes to the total power depends on the dipole orientation [22], shown in Fig. 3. The relative contribution can be explained in terms of the excitation fields, using Eq. (2). For example, a z-oriented dipole couples strongly into the modes with a large z-component electric field, i.e., TM radiated modes of the fiber. Note that the radiated power is normalized to the total radiated dipole power from the telluride glass, which represents the Purcell factor of the coupled system. The position of these peaks overlaps with the position of the TE-WGM resonances (blue triangles) of a two-dimensional (2D) microdisk calculated independently by solving Maxwell's equations for a 2D circular disk with a diameter equal to that of the fiber.

The insets in Fig. 3 represent the normalized fields (magnetic for Figs. 3(a) and 3(b) and electric for Fig. 3(c)) at the cross section of the fiber at the position of (8,0) WGM for each case. These insets are calculated using commercially available numerical software CST microwave studio. We demonstrated that the radiation peaks are due to contribution from a very small range of propagation constants close to zero implying that there is a very small contribution from non-transverse propagating modes (skew modes) and it almost radiated in the transverse plane. We also demonstrated that Q-factor and modal volume both increase exponentially as functions of core diameter, the Q-factor increases faster, which results in an

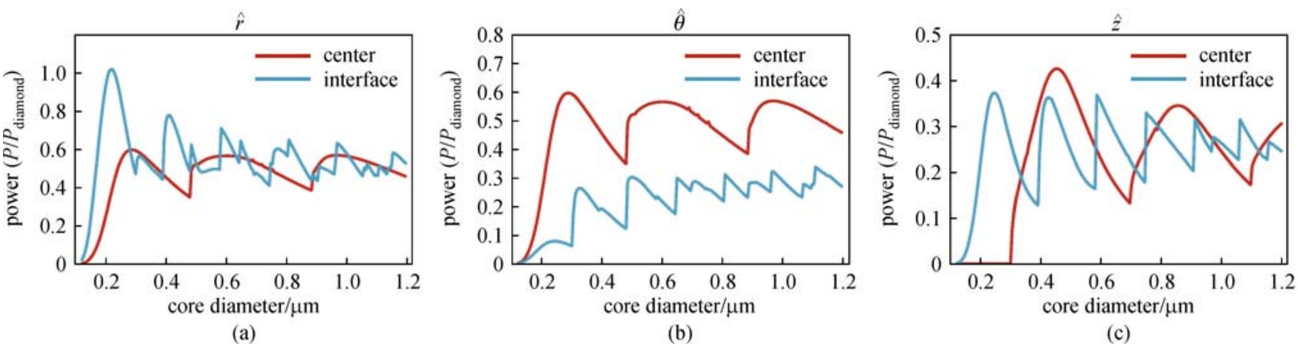

Fig. 2 Power captured into the guided modes vs. core diameter for a tellurite core and air clad fiber excited by an electric dipole emitting at 700 nm in the core center (red) and on the cladding (blue) interface. (a) Radially, (b) azimuthally, and (c) longitudinally oriented dipole. Power is normalized to the total power emitted in a bulk diamond material. All adapted from Ref. [18]

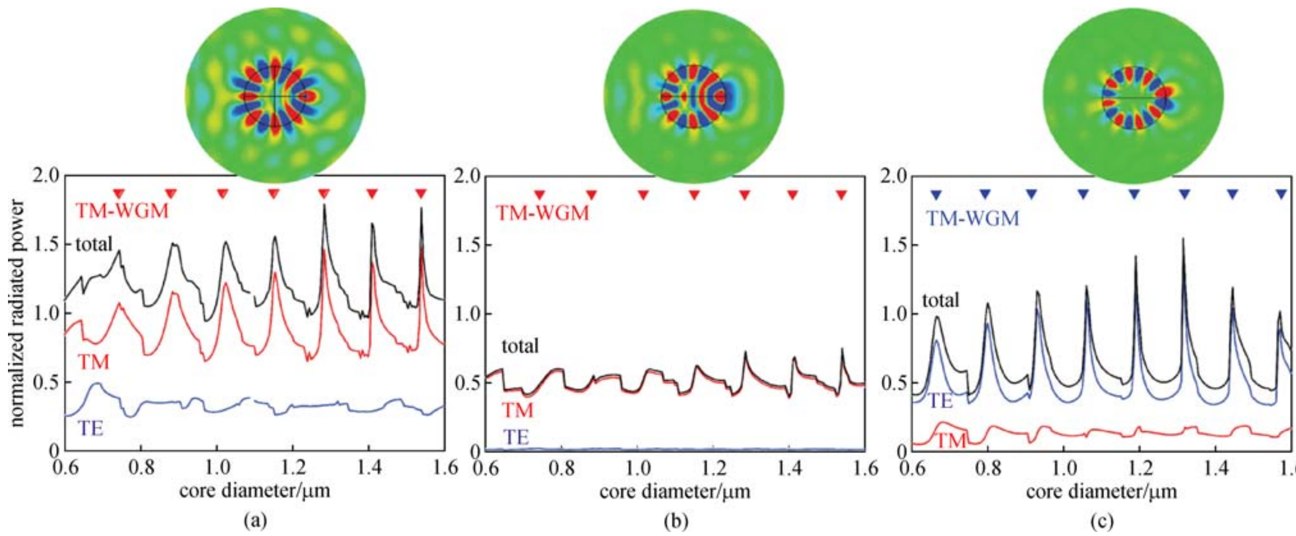

Fig. 3 Normalized radiated power (total, TE and TM) of a coupled system when excitation is oriented (a) radially, (b) azimuthally, and (c) longitudinally. Power is normalized to the total power emitted in a bulk tellurite glass. The position of the resonances of 2D TE- and TM-WGMs is shown respectively with blue and red triangles. The insets represent the normalized magnetic field ((a) and (b)) and electric field ((c)) of (8,0) WGM for each case, which is the peak just before 1.2 μm in each case. Adapted from Ref. [22]

exponential increase of the Purcell factor similar to what has also been observed in two dimensional planar microcavities [2].

High Q-factors of the radiation peaks of the dipole-fiber system indicates that this configuration can also be used for refractive index sensing applications. We demonstrated that the sensitivity in this coupled system increases exponentially for higher order resonance modes and can be used as a platform for ultra-sensitive refractive index sensing (possibility of detecting $\delta n \approx 5 \times 10^{-10}$ at (29,0) resonance peak) [2]. The distinguished point of the dipole-fiber system from other refractive index sensors (micro-capillaries) is the selective coupling of a dipole emission to those WGMs that have almost zero skew components ($\beta = 0$) [2].

5 A new platform for metadevices

In Section 4, we considered the effect of dipole emission into radiation modes of the optical fiber, where strong resonance peaks are observed due to formation of WGMs at the fiber cross section [2,22]. In this section, we reveal that a dipole placed near an optical fiber can produce strong magnetic response. We focus on the first radiation peak of coupled system and theorectically demonstrate that the dipole orientation determines the nature of the resonance response (electric or magnetic) of the system [22,23]. This nanophotonic system opens up new possibilities to develop low-dimensional nanodevices with enhanced magnetic response.

The contribution of each of these TE- and TM-like modes into the total power of the first peak depends on the dipole orientation, shown in Fig. 3. For azimuthally and longitudinally oriented dipole emission there exist strong TM and TE-like modes contribution respectively, while for radially oriented dipole both TE and TM have relatively strong contribution and the relative ratio dependent of the refractive index of the core [23]. To determine the nature of the first resonance, we used the electromagnetic multipole expansion and decomposed the fields radiated in terms of electric and magnetic multipoles. Once the radiated/scattered electric field is known, the following equations can be used to determine the decomposition coefficients [25,26]:

$$a_{\mathrm{E}}(l,m) = \frac{(-\mathrm{i})^{l+1} kr}{h_l^{(1)}(kr) E_0 [\pi(2l+1) l(l+1)]^{1/2}} \int_0^{2\pi} \int_0^{\pi} Y_{lm}^*(\theta,\phi) \hat{\boldsymbol{r}} \cdot \boldsymbol{E}_{\mathrm{s}}(\boldsymbol{r}) \sin\theta \mathrm{d}\theta \mathrm{d}\phi, \tag{4}$$

$$a_{\mathrm{M}}(l,m) = \frac{(-\mathrm{i})^{l}}{h_l^{(1)}(kr) E_0 [\pi(2l+1)]^{1/2}} \int_0^{2\pi} \int_0^{\pi} \boldsymbol{X}_{lm}^*(\theta,\phi) \cdot \boldsymbol{E}_{\mathrm{s}}(\boldsymbol{r}) \sin\theta \mathrm{d}\theta \mathrm{d}\phi, \tag{5}$$

where $a_E(l,m)$, and $a_{\mathrm{M}}(l,m)$ respectively represent the amplitude of electric and magnetic (l,m) mulitpoles, X_{lm} and $h_l^{(1)}$ are the normalized vector spherical harmonics and the spherical Hankel functions of the first kind, respectively, where l and m are respectively the degree and order of the harmonics. Also E_0 and E_{s} are respectively the excitation and scattered/system electric field, and k is free

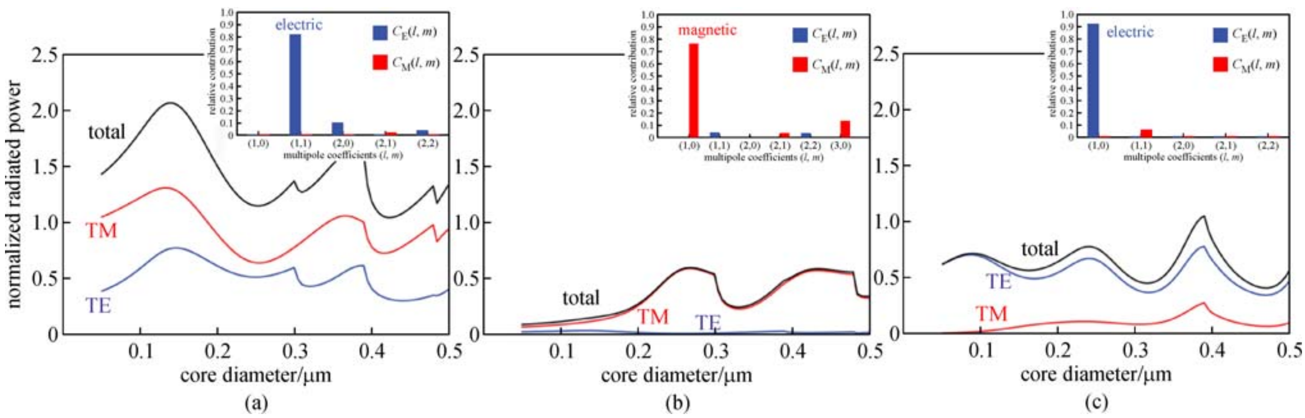

Fig. 4 First two-three peaks of normalized radiated power (total in black, TE in blue and TM in red) of a coupled system when excitation is oriented (a) radially, (b) azimuthally, and (c) longitudinally. Power is normalized to the total power emitted in a bulk tellurite glass. The insets represent relative contribution of multipole coefficients (l,m) in the total energy of the system. Adapted from Ref. [22]

space wavevector. Using decomposition, we have demonstrated that the first peak of azimuthally oriented dipole, which has mainly TM-like component, has a strong magnetic dipole response $a_M(0,1)$, while the other two orientations have electric dipole or higher order multipoles (in case of radial electric dipole). Once the multipole coefficients are determined, one can easily calculate the relative contribution of each decomposed component in total energy of the system as follows [25]:

$$C_{E,M}(l,m) = \pi(2l+1)|a_{E,M}(l,m)|^2/(k^2 W_s), \qquad (6)$$

where W_s is the total radiated energy in the system. The relative contribution of each decomposed component in total energy of the system are shown in the insets of Fig. 4. For a longitudinal dipole excitation, the energy couples predominantly in the $C_E(1,0)$ component; representing the system behaves as an enhanced electric dipole along. For a radial dipole excitation, most of the energy also couples into electric mulitpoles (dipole $C_E(1,1)$ and quadrupole $C_E(2,0)$). This is while for an azimuthal dipole excitation there exist a strong contribution (more than 75%) from $C_M(1,0)$, i.e., a magnetic dipole moment. This implies that the electric response of the system is suppressed preferentially while its magnetic response is enhanced (more than 2 orders of magnitude) [22]. This strong magnetic response is observed in a system with a relatively moderate refractive index. We believe these results will pave the way to developing novel optical fiber devices with a large induced magnetic response.

6 Conclusion

Here, we summarized our work on the interaction of optical fibers with point source, i.e., electric dipole or quantum emitter. We explained the theoretical modeling used to calculate power coupled into guided and radiation modes of the coupled system followed by three different application of this system depending to the relative position and orientation of the dipole and the core diameter of the optical fiber. We demonstrated that such a system can be a guided single photon source when the optical fiber is doped with diamond nanoparticles, a platform for ultra-sensitive refractive index sensing (possibility of detecting $\delta n \approx 5 \times 10^{-10}$) due to the excitation of high quality factor WGMs, and a platform for developing novel optical fiber based metadevices with a large induced magnetic response.

Acknowledgements S. Atakaramians acknowledges the support of Australian Research Council (ARC) under the Discovery Early Career Project Award number DE140100614. T. M. Monro acknowledges the support of ARC Georgina Sweet Laureate Fellowship.

References

1. Vahala K JOptical microcavities. Nature, 2003, 424(6950): 839–846
2. Afshar V S, Henderson M R, Greentree A D, Gibson B C, Monro T MSelf-formed cavity quantum electrodynamics in coupled dipole cylindrical-waveguide systems. Optics Express, 2014, 22(9): 11301–11311
3. Hall J M M, Reynolds T, Henderson M R, Riesen N, Monro T M, Afshar S. Unified theory of whispering gallery multilayer microspheres with single dipole or active layer sources. Optics Express, 2017, 25(6): 6192–6214
4. Chew H, McNulty P J, Kerker M. Model for Raman and fluorescent scattering by molecules embedded in small particles. Physical Review A, 1976, 13(1): 396–404
5. Arnold S, Khoshsima M, Teraoka I, Holler S, Vollmer F. Shift of whispering-gallery modes in microspheres by protein adsorption. Optics Letters, 2003, 28(4): 272–274
6. Quan H, Guo Z. Simulation of whispering-gallery-mode resonance shifts for optical miniature biosensors. Journal of Quantitative Spectroscopy & Radiative Transfer, 2005, 93(1–3): 231–243

7. Guo Z, Quan H, Pau S. Near-field gap effects on small microcavity whispering-gallery mode resonators. Journal of Physics D, Applied Physics, 2006, 39(24): 5133–5136
8. Imakita K, Shibata H, Fujii M, Hayashi S. Numerical analysis on the feasibility of a multi-layered dielectric sphere as a three-dimensional photonic crystal. Optics Express, 2013, 21(9): 10651–10658
9. Li M, Wu X, Liu L, Xu L. Kerr parametric oscillations and frequency comb generation from dispersion compensated silica micro-bubble resonators. Optics Express, 2013, 21(14): 16908–16913
10. Farnesi D, Barucci A, Righini G C, Conti G N, Soria S. Generation of hyper-parametric oscillations in silica microbubbles. Optics Letters, 2015, 40(19): 4508–4511
11. Ruan Z, Fan S. Superscattering of light from subwavelength nanostructures. Physical Review Letters, 2010, 105(1): 013901
12. Agio M. Optical antennas as nanoscale resonators. Nanoscale, 2012, 4(3): 692–706
13. Novotny L, van Hulst N. Antennas for light. Nature Photonics, 2011, 5(2): 83–90
14. Bharadwaj P, Deutsch B, Novotny L. Optical antennas. Advances in Optics and Photonics, 2009, 1(3): 438–483
15. Kivshar Y, Miroshnichenko A. Meta-optics with Mie resonances. Optics and Photonics News, 2017, 28(1): 24–31
16. Zheludev N I, Kivshar Y S. From metamaterials to metadevices. Nature Materials, 2012, 11(11): 917–924
17. Snyder A W, Love J. Optical Waveguide Theory. 1st ed. London: Chapman and Hall Ltd, 1983
18. Henderson M R, Afshar V. S, Greentree A D, Monro T M. Dipole emitters in fiber: interface effects, collection efficiency and optimization. Optics Express, 2011, 19(17): 16182–16194
19. Henderson M R, Gibson B C, Ebendorff-Heidepriem H, Kuan K, Afshar V S, Orwa J O, Aharonovich I, Tomljenovic-Hanic S, Greentree A D, Prawer S, Monro T M. Diamond in tellurite glass: a new medium for quantum information. Advanced Materials, 2011, 23(25): 2806–2810
20. Ebendorff-Heidepriem H, Ruan Y, Ji H, Greentree A D, Gibson B C, Monro T M. Nanodiamond in tellurite glass Part I: origin of loss in nanodiamond-doped glass. Optical Materials Express, 2014, 4 (12): 2608–2620
21. Ruan Y, Ji H, Johnson B C, Ohshima T, Greentree A D, Gibson B C, Monro T M, Ebendorff-Heidepriem H. Nanodiamond in tellurite glass Part II: practical nanodiamond-doped fibers. Optical Materials Express, 2015, 5(1): 73–87
22. Atakaramians S, Miroshnichenko A E, Shadrivov I V, Mirzaei A, Monro T M. Kivshar Y S, Afshar V S. Strong magnetic response of optical nanofibers. ACS Photonics, 2016, 3(6): 972–978
23. Atakaramians S, Miroshnichenko A E, Shadrivov I V, Monro T M. Kivshar Y S, Afshar V. S. Dipole-fiber systems: radiation field patterns, effective magnetic dipoles, and induced cavity modes. In: Proceedings of SPIE 9668, Micro + Nano Materials, Devices, and Systems, 2015, 96683J
24. Fussell D P, McPhedran R C, Martijn de Sterke C. Decay rate and level shift in a circular dielectric waveguide. Physical Review A, 2005, 71(1): 013815
25. Jackson J. Classical Electrodynamics. 3rd ed. New York: John Wiley & Sons, Inc., 1998
26. Grahn P, Shevchenko A, Kaivola M. Electromagnetic multipole theory for optical nanomaterials. New Journal of Physics, 2012, 14 (9): 093033

Dr. **Shaghik Atakaramians** is a Scientia Fellow at the Unieristy of New South Wales (UNSW), Syndey. She joined the School of Electrical Engineering and Telecommunicates at UNSW in June 2017 and leads terahertz activities within the School.

Shaghik Atakaramians was awarded ARC Discovery Early Career Researcher Award (DECRA) in 2014 on terahertz metamaterial waveguides. She worked at the Institute of Photonics and Optical Science (IPOS) at the University of Sydney from 2011 to 2017 as a postdoctoral and research fellow. She also worked for The Centre for Ultrahigh bandwidth Devices for Optical Systems (CUDOS) from 2012 to 2014.

Shaghik Atakaramians received her Ph.D. degree in Electrical & Electronic Engineering with a Certificate of Merit from the Dean in 2011. Her PhD thesis has won the Gertrude Rohan Memorial Prize and 2011 University Doctoral Research Medal for outstanding research.

Prof. **Tanya M. Monro** took up the role of Deputy Vice Chancellor Research and Innovation in November 2014.

The ARC Georgina Sweet Laureate Fellow at the University of South Australia, Prof. Monro was the inaugural Director of the Institute for Photonics and Advanced Sensing (IPAS) from 2008 to 2014 and was also the inaugural Director for the ARC Centre of Excellence for Nanoscale BioPhotonics (CNBP) at the University of Adelaide. Her research is in the field of photonics, with a focus on sensing, lasers and new classes of optical fibres.

Prof. Monro obtained her Ph.D. degree in Physics in 1998 from The University of Sydney, for which she was awarded the Bragg Gold Medal. In 2000, she received a Royal Society University Research Fellowship at the Optoelectronics Research Centre at the University of Southampton.

Prof. Monro is a Fellow of the Australian Academy of Science (AAS), the Australian Academy of Technological Sciences and Engineering (ATSE), the Optical Society of America (OSA) and the Australian Institute of Physics. She is a member of the Prime Minister's Commonwealth Science Council (CSC), and a Board Member of the Commonwealth Science and Industrial Research Organisation (CSIRO), the South Australian Defence Advisory Board, and the South Australian Economic Development Board.

Tanya's awards include: Eureka Prize for Excellence in Interdisciplinary Scientific Research, the Bragg Gold Medal (best Physics PhD in Australia), South Australia's "Australian of the Year", Scopus Young Researcher of the Year, South Australian Scientist of the Year, and the Prime Minister's Malcolm McIntosh Prize for Physical Scientist of the Year.

A/Prof. **Shahraam AfsharV.** received his Ph.D. degree in Physics, Laser and Nonlinear Optics, from the University of Adelaide in 2001. From 1998 to 2001, he held a lecturer position at The University of Adelaide.

In 2001, he joined the fibre optics group at The University of Ottawa, where he worked on distributed strain and temperature sensors based on Brillouin scattering in optical fibers. In 2003, he received the NCIT fellowship from National Capital Institute of Telecommunication, Canada to work on Brillouin scattering in photonic crystal fibres.

In 2005, he joined the Centre of Expertise in Photonics (CoEP) at the University of Adelaide, which later on formed into the Institute for Photonics and Advanced Sensing (IPAS). Since 2015, he is an Associate Professor of Photonics at School of Engineering of University of South Australia. His research interests cover different linear and nonlinear processes in optical waveguides including fiber optic sensors, nonlinear fibre optics, and strong light-matter interactions in subwavelength fibers.